EXECUTIVE SUMMARY

Reactive Electrochemical Membrane (REM) Reactors for the Oxidation of PFAS-Impacted Water

SERDP Project ER18-1491

MAY 2020

Brian Chaplin
Amisha Shah
University of Illinois at Chicago

Distribution Statement A
This document has been cleared for public release

SERDP
DOD ▪ EPA ▪ DOE

This report was prepared under contract to the Department of Defense Strategic Environmental Research and Development Program (SERDP). The publication of this report does not indicate endorsement by the Department of Defense, nor should the contents be construed as reflecting the official policy or position of the Department of Defense. Reference herein to any specific commercial product, process, or service by trade name, trademark, manufacturer, or otherwise, does not necessarily constitute or imply its endorsement, recommendation, or favoring by the Department of Defense.

EXECUTIVE SUMMARY

Project: ER18-1491

TABLE OF CONTENTS

Page

1.0 INTRODUCTION 1
2.0 OBJECTIVES 1
3.0 TECHNICAL APPROACH 2
4.0 RESULTS AND DISCUSSION 2
4.1 OVERVIEW OF RESULTS 2
4.1.1 Milestone 1: Synthesis of sorbent-loaded REMs with high sorption capacities for PFAS (> 10 mg/g of sorbent). 2
4.1.2 Milestone 2: Demonstrate the ability of REMs to remove PFAS from an initial concentration of > 400 µg L^{-1} to below the treatment goal of 70 ng L^{-1} in synthetic/real groundwater samples. 3
4.1.3 Milestone 3: Determination of the most energy efficient operational strategy for PFAS removal in groundwater. 3
4.1.4 Milestone 4: Determination of the energy costs for achieving the 70 ng L^{-1} treatment goal in PFAS-contaminated groundwater with a target energy usage of < 2.0 kWh m-3 of water treated. 3
4.2 PFOA AND PFOS OXIDATION IN SYNTHETIC SOLUTIONS 3
4.3 PFAS OXIDATION IN GROUNDWATER SAMPLES 6
4.4 ENERGY REQUIREMENTS 9
5.0 RESEARCH AND BENEFITS 10
6.0 LITERATURE CITED 10
APPENDIX A COMPARISON OF ENERGY CONSUMPTION OF REPORTED TECHNOLOGIES FOR PFOA/PFOS DEGRADATION 14

LIST OF FIGURES

Page

Figure E1. (a) Concentration Profile of Permeate during the Oxidation of PFOA and PFOS on Ti4O7 REM. (b) Concentration of PFHpA Formed from PFOA Oxidation. 5
Figure E2. (a) Concentration Profile of Permeate, (b) Removal Rate of PFOA/PFOS During the Oxidation on Ti4O7 REM at Different Membrane Fluxes. 6
Figure E3. PFAS and Total F Removal in GW1 Sample as a Function of Cell Potential. 8
Figure E4. Comparison of Electrochemical Oxidation of PFAS in GW2 in Single-Pass Versus Recycle Modes. 8
Figure E5. Percent Removal of PFAS Compounds in GW2. 9

LIST OF TABLES

Page

Table E1. General Water Quality Analyses for Groundwater Samples..... 7

ACRONYMS AND ABBREVIATIONS

AFFFs	aqueous film forming foam
BDD	boron-doped diamond
COD	chemical oxidant demand
DoD	U.S. Department of Defense
EPA	U.S. Environmental Protection Agency
GAC	granular activated carbon
GW1	groundwater 1
GW2	groundwater 2
IDW	investigation-derived waste
kWh	kilowatt hour
LCA	life cycle assessment
LC-MS	liquid chromatography/mass spectroscopy
LMH	liters per meter squared per hour
MWCNTs	multi-walled carbon nanotubes
OCP	open circuit potential
PAC	powdered activated carbon
PFAS	per- and polyfluoroalkyl substances
PFBS	perfluorobutanesulfonic acid
PFOA	perfluorooctanoic acid
PFOS	perfluorooctanesulfonic acid
PFHxS	perfluorohexane sulfonate
PFHpA	perfluoroheptanoic acid
PFNA	perfluornonanoic acid
REM	reactive electrochemical membrane
SERDP	Strategic Environmental Research and Development Program
SHE	standard hydrogen electrode
UCMR-3	third unregulated contaminant monitoring rule
UV	ultraviolet

ACKNOWLEDGEMENTS

The project thanks Dr. Todd DeJournett, Dr. James Wang, and David Sherman from Geosyntec Consultants for procuring groundwater samples and Jason Speicher from Willow Grove Naval Base for allowing us to collect groundwater samples for this project. Finally, the project thanks Dr. Todd DeJournett and Dr. James Wang for useful discussions regarding site remediation.

1.0 INTRODUCTION

Per- and polyfluoroalkyl substances (PFAS), including perfluorooctanoic acid (PFOA) and perfluorooctanesulfonic acid (PFOS), originating from aqueous film forming foams (AFFFs) pose a serious human health risk. Therefore, the U.S. Environmental Protection Agency (EPA) has established a 70 ng L^{-1} lifetime health advisory level for PFOA and PFOS (EPA 2016), and several states have set even lower standards (e.g., California and New Jersey: 14 ng L^{-1} for PFOA and 13 ng L^{-1} for PFOS) (ASDWA 2020). The removal of these compounds from groundwater is complicated by low volatility and general lack of reactivity to biodegradation and traditional oxidative treatment processes (e.g., advanced oxidation processes, ultraviolet (UV) photolysis) (Schroder et al. 2005). As a result, treatment strategies have mainly used granular activated carbon (GAC) and other sorbents for PFAS removal (Carter and Farrell 2010; Zhang et al. 2016; Zhao et al. 2011; Eschauzier et al. 2012; Pramanik et al. 2015; Yao et al. 2014; Yu et al. 2009). However, studies have found that desorption of PFAS from GAC (and other sorbents) was nearly irreversible using conventional regeneration methods (Carter and Farrell 2010), which greatly increases the costs associated with adsorbent-based treatment strategies. PFAS-contaminated groundwater also often contains other co-contaminants, including hydrocarbon surfactants originating from the AFFFs, chlorinated solvents, solvent stabilizers, and fuel components. Therefore, effective remediation technologies should be capable of the simultaneous removal of this diverse group of contaminants, which will be beneficial for on-site treatment of investigation-derived wastes (IDWs).

Here, the project team describes an innovative, destructive treatment strategy for the remediation of PFAS-contaminated IDWs. The project team has designed a novel reactive electrochemical membrane (REM) system that is capable of electrochemical destruction of PFAS and associated co-contaminants. A successful proof of concept of the REM technology will be transformative for groundwater remediation, as it will show that a single, compact technology is capable of providing cost-effective remediation of PFAS in groundwater samples. However, there are several technological challenges that must be met in order to establish proof of concept. These challenges include: 1) demonstration of destructive PFAS removal in IDW water samples to < 70 ng L^{-1}; 2) optimization of the operational mode; and 3) low energy consumption compared to other destructive treatment methods. Overcoming these challenges will indicate that the REM is a viable PFAS remediation technology, where additional research and development focused on scale-up and pilot testing could lead to large-scale treatment systems for site-wide remediation.

2.0 OBJECTIVES

The proposed research was focused on the development of a novel REM treatment system for the remediation of PFAS in liquid samples that were generated from subsurface investigations of PFAS contamination at groundwater sites, known as IDW. Thus, this research is directly in line with the objectives of the Strategic Environmental Research and Development Program (SERDP) Statement of Need (ERSON-18-L1). The REM technology was developed with consideration towards technical effectiveness, cost effectiveness, compactness, and mobility of the treatment system. The completed Limited Scope project has produced proof-of-concept data that indicates that a REM-based remediation strategy is a viable option for the treatment of IDW liquid samples.

The overall objective of this work was to utilize a cost-effective REM for the removal of PFAS from liquid IDW samples collected at contaminated groundwater sites. Specific technical objectives associated with this project included: 1) development of REMs for destructive PFAS removal in IDW water samples to < 70 ng L^{-1}; 2) determination of the optimal operational mode; and 3) calculation of energy requirements for the REM-based system for comparison to other technologies. These objectives were accomplished in this work and thus the project team has established proof of concept that the REM system is a viable technology for PFAS remediation. Therefore, the project team is seeking a follow-on project to develop a pilot-scale treatment system to test the long-term effectiveness of PFAS remediation in IDW samples. Deliverables of this follow-on research include: 1) a scaled-up optimized reactor; 2) durable REMs with a projected lifetime of > 10 years; and 3) cost and life cycle assessments (LCAs) for comparison to other technologies. A specific focus of the follow-on research will be to characterize short-chain PFAS that are produced during REM treatment and to either optimize REM operational parameters to eliminate these products or couple the REM to other post treatment strategies. These deliverables will allow practitioners to evaluate this new technology for implementation at PFAS-contaminated U.S. Department of Defense (DoD) sites, with the goal of creating on-site disposal options to lower the cost of site management.

3.0 TECHNICAL APPROACH

The work performed during this project consisted of REM synthesis, a series of bench-scale experimental studies, and a preliminary energy cost assessment. The six PFAS compounds on the EPA's third unregulated contaminant monitoring rule (UCMR-3) list were investigated, which included PFOA, PFOS, perfluorononanoic acid (PFNA), perfluorohexanesulfonic acid (PFHxS), perfluoroheptanoic acid (PFHpA), and perfluorobutanesulfonic acid (PFBS). A specific focus on treatment of PFOS and PFOA was made, which allowed comparison of results to the existing literature. Experimental parameters that were explored included: 1) adsorption capacity; 2) necessary residence time in the reactor; 3) reactor operational mode; and 4) energy usage (kilowatt hour (kWh) m^{-3} per log removal of PFAS).

4.0 RESULTS AND DISCUSSION

4.1 OVERVIEW OF RESULTS

The Limited Scope project had four specific milestones which were used to determine if proof of concept was met. These four milestones and a brief discussion of the primary results are discussed below:

4.1.1 Milestone 1: Synthesis of sorbent-loaded REMs with high sorption capacities for PFAS (> 10 mg/g of sorbent).

Results: Sorbed-loaded REMs were synthesized containing multi-walled carbon nanotubes (MWCNTs) and powdered activated carbon (PAC). Although the addition of these sorbent materials resulted in a significant increase in the adsorption of PFAS, they were found to be unstable during anodic polarization. Therefore, the anticipated strategy of using the sorbent-loaded REMs for a "trap and zap" treatment approach was not explored in further detail. However, preliminary experiments were conducted that indicates that electrosorption of PFOA on to the MWCNT-REM was significantly higher than the

REM. These results suggest that an electrosorption step may be included before electrochemical oxidation to concentrate PFAS, but the concept was not explored in detail as it was not a primary focus of the project.

4.1.2 Milestone 2: Demonstrate the ability of REMs to remove PFAS from an initial concentration of > 400 µg L^{-1} to below the treatment goal of 70 ng L^{-1} in synthetic/real groundwater samples.

Results: This milestone was achieved in both synthetic samples for PFOA and PFOS and for real groundwater samples for a mixture of PFAS.

4.1.3 Milestone 3: Determination of the most energy efficient operational strategy for PFAS removal in groundwater.

Results: The most efficient operational strategy for PFAS removal from groundwater was found to be a recycle-mode with a high permeate flux. This mode of operation could achieve the treatment goal stated in **Milestone 1** for a mixture of PFAS present in groundwater.

4.1.4 Milestone 4: Determination of the energy costs for achieving the 70 ng L^{-1} treatment goal in PFAS-contaminated groundwater with a target energy usage of < 2.0 kWh m-3 of water treated.

Results: An energy usage of 2.9 kWh m^{-3} per log removal of PFAS was measured for the mixture of PFAS in groundwater with the REM operated in recycle-mode. Although this value is slightly higher than the goal, further optimization of the reactor design (e.g., electrode spacing, fluid dynamics) should allow much lower energy consumptions to be realized.

Overall, proof of concept was established, and the project team is confident that further research into reactor design and process optimization will lead to achieving the energy usage goal (**Milestone 4**). It should be noted that the reported energy usage values in the work are the lowest reported for electrochemical oxidation and approximately an order of magnitude lower than those reported for other destructive technologies (i.e., ultrasonication, photocatalysis, vacuum UV photolysis, microwave-hydrothermal decomposition). The complete results of this project are discussed below in further detail.

4.2 PFOA AND PFOS OXIDATION IN SYNTHETIC SOLUTIONS

Work in this section focused on **Milestone 2: Demonstrate the ability of REMs to remove PFAS from an initial concentration of > 400 µg L^{-1} to below the treatment goal of 70 ng L^{-1} in synthetic/real groundwater samples.**

The results shown in this section were recently published in *Environmental Science and Technology Letters* (Le et al. 2019). PFOA and PFOS were chosen as model PFAS to test the effectiveness of the REM for electrochemical oxidation. The effect of the applied anodic potential

on PFOA/PFOS degradation using the REM at a flux of 240 liters per meter squared per hour (LMH) is shown in **Figure E1**. Oxidation experiments for PFOA were performed at the open circuit potential (OCP) to 3.3 V/standard hydrogen electrode (SHE) (**Figure E1a**) and for PFOS at the OCP to 3.6 V/SHE (**Figure E1b**). Nearly complete removal was achieved for both compounds in a single pass through the REM with residence times of 11.3 s (3.3 V/SHE for PFOA and 3.6 V/SHE for PFOS).

The maximum removal for PFOA was achieved at 3.3 V/SHE with a 4.7 ± 0.05-log removal and permeate concentrations were below the analytical detection limit (86 ng L^{-1}). The maximum removal for PFOS was achieved at 3.6 V/SHE with a 5.2 ± 0.02-log removal, and permeate concentrations were below the analytical detection limit (35 ng L^{-1}). The detection limits for PFOA/PFOS were on order with the 70 ng L^{-1} lifetime health advisory level established by EPA (EPA 2016), which achieved the goal set forth by **Milestone 2**. However, the permeate concentrations were still higher than standards set forth by several states (e.g., California and New Jersey: 14 ng L^{-1} for PFOA and 13 ng L^{-1} for PFOS) (ASDWA 2020).

The formation of F^- ions was used to calculate the defluorination ratio of PFOA/PFOS (i.e., [F^- formed]/[F in initial PFAS]*100) and values were up to 75.3 ± 4.7 % for PFOA (**Figure E1c**) and 68.9 ± 2.7 % for PFOS (**Figure E1d**). The total fluorine mass balance was calculated (i.e., $\{[F^-]_{\text{in solution}} + [F]_{\text{in PFAS, J}} / [F]_{\text{in PFAS, initial}}\}$) and ranged between 68.1 ± 4.1 to 99.7 ± 0.3 % for PFOA (**Figure E1c**) and between 67.2 ± 4.1 to 99.8 ± 0.2 % for PFOS (**Figure E1d**). The only fluorocarbon product detected during experiments was PFHpA during PFOA oxidation (**Figure E1b**). The maximum concentration of PFHpA formed at a potential of 2.6 V/SHE and decreased at higher potentials, which was attributed to a lowering of the activation energy for PFHpA oxidation at higher potentials. The fact that the mass balance was < 100% indicates that shorter chain volatile PFAS products likely formed, which were not analyzed by liquid chromatography/mass spectroscopy (LC-MS) (Niu et al. 2012; Niu et al. 2013).

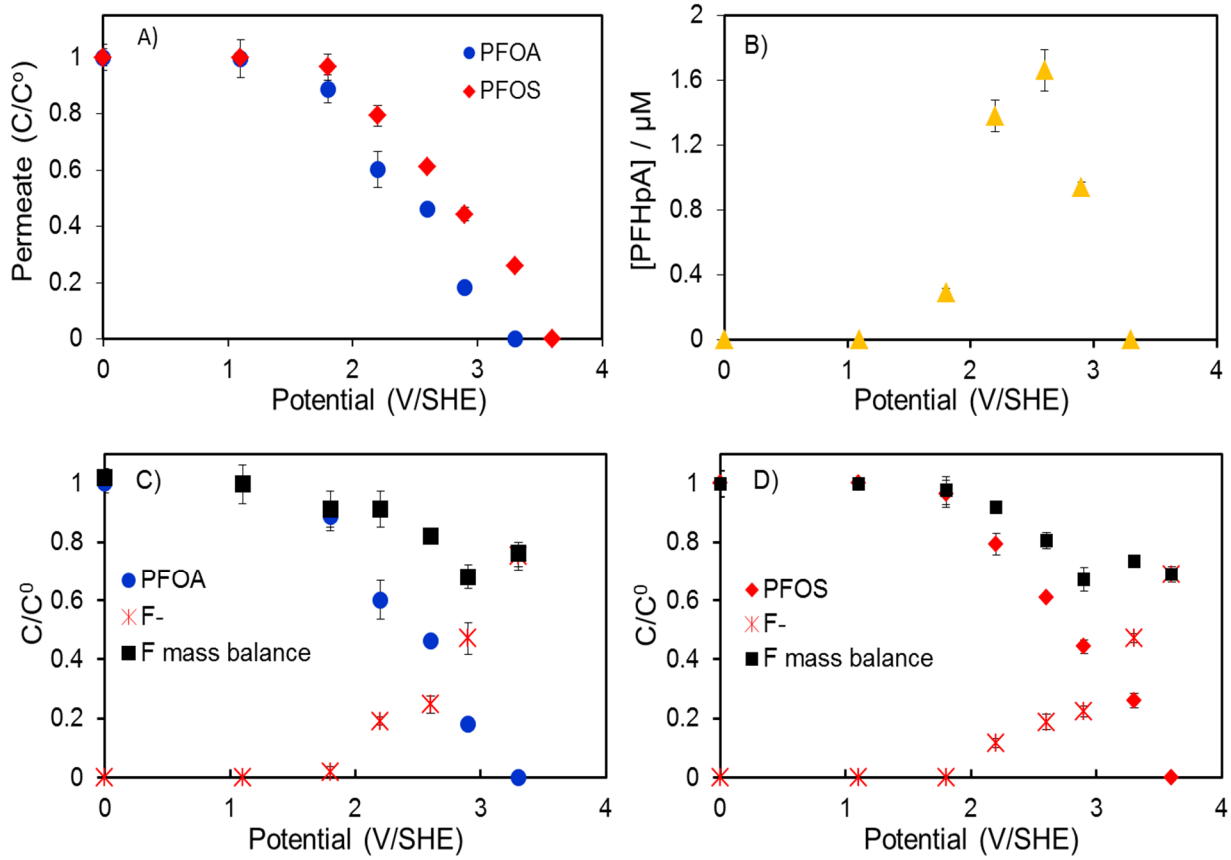

Figure E1. (a) Concentration Profile of Permeate during the Oxidation of PFOA and PFOS on Ti4O7 REM. (b) Concentration of PFHpA Formed from PFOA Oxidation.

Fluoride Mass Balance as a Function of Potential for (c) PFOA, and (d) PFOS at J = 240 LMH. (Electrolyte = 100 mM K2HPO4). Concentrations were normalized by initial PFAS concentration. Error bars represent standard deviations about mean values and are contained within data points for some data (Le et al. 2019).

Results for the electrochemical oxidation of PFOA/PFOS at a constant anodic potential of 2.9 V/SHE and with different membrane fluxes (J = 36 to 960 LMH) are shown in **Figure E2**. These membrane fluxes gave residence times between 75 to 2.8 s. The highest conversions for both compounds were found at J = 36 LMH, which again achieved approximately 5-log removal for both compounds (liquid residence time = 75 s). **Figure E2b** contains the calculated PFAS removal rates as a function of J. The maximum removal rates for PFOA/PFOS were obtained at J = 720 LMH, with R_r = 3415 ± 203 µmol m^{-2} h^{-1} for PFOA and R_r = 2436 ± 106 µmol m^{-2} h^{-1} for PFOS. Reaction rate constants were also calculated based on the conversion of PFOA/PFOS as a function of liquid residence time in the REM. Results indicated that the reactions were pseudo first-order, with surface area normalized observed rate constants (k_{obs}) of 1.3 x 10^{-4} m s^{-1} for PFOA and 4.4 x 10^{-5} m s^{-1} for PFOS. These k_{obs} values were over an order of magnitude higher than previously reported results with Ti_4O_7 and boron-doped diamond (BDD) anodes (Ochiai et al. 2011; Lin et al. 2018). These significantly improved results were attributed to the flow-through mode operation, which enhanced mass transfer and utilized the high specific surface area of the REM (i.e., 1.3 x 10^6 m^{-1}).

In addition, non-normalized observed reaction rate constants for this data were calculated as 607 h^{-1} for PFOA and 210 h^{-1} for PFOS. These values are more than two orders of magnitude higher than those reported by other destructive technologies (i.e, ultrasonication, photocatalysis, vacuum UV photolysis, microwave-hydrothermal decomposition) (Vecitis et al. 2008; Lee et al. 2009; Chen et al. 2016; Jin and Zhange 2015).

The defluorination ratios as a function of *J* were between 20.3% ± 3.8 at 960 LMH to 81.4% ± 3.2 at 36 LMH for PFOA (**Figure E2c**) and between15.5 ± 2.2 % at 960 LMH to 72.9 ± 3.1 % at 36 LMH for PFOS (**Figure E2d**). The total fluorine mass balance ranged between 74.1 ± 0.07 to 98.6 ± 0.16 % for PFOA (**Figure E2c**) and between 71.7 ± 5.8 % to 93.8 ± 4.1 % for PFOS (**Figure E2d**).

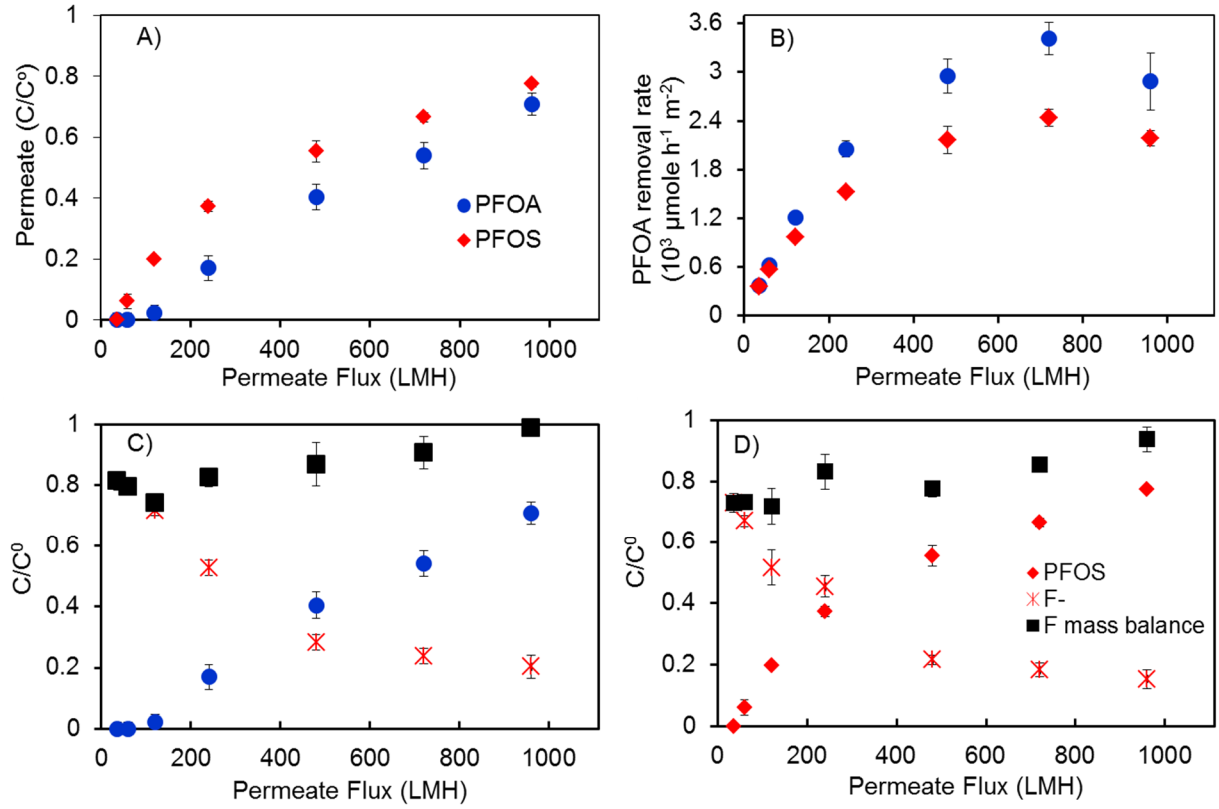

Figure E2. (a) Concentration Profile of Permeate, (b) Removal Rate of PFOA/PFOS During the Oxidation on Ti4O7 REM at Different Membrane Fluxes.

Fluoride Mass Balance as a Function of Membrane Flux of (c) PFOA, and (d) PFOS (V anode = 2.9 V/SHE, Electrolyte = 100 mM K2HPO4). Error bars represent standard deviations about mean values and are contained within data points for some data (Le et al. 2019).

4.3 PFAS OXIDATION IN GROUNDWATER SAMPLES

Work in this section focused on addressing **Milestones 2 and 3**.

Milestone 2: Demonstrate the ability of REMs to remove PFAS from an initial concentration of > 400 µg L^{-1} to below the treatment goal of 70 ng L^{-1} in synthetic/real groundwater samples.

Milestone 3: Determination of the most energy efficient operational strategy for PFAS removal in groundwater.

Two groundwater samples (groundwater 1 (GW1) and groundwater 2 (GW2)) were treated with the REMs. The general water quality analyses for these samples are shown in **Table E1**. The GW1 sample was collected by Geosyntec Consultants from a client's site in Jacksonville, Florida and did not contain detectable concentrations of PFAS. This sample was spiked with the six different PFAS at concentrations between 1.0 to 2.5 µM. These initial concentrations are shown in **Figure E3** (OCP/Feed data). This experiment was conducted at low flux (J = 60 LMH), which gave a hydraulic residence time of t_r = 45 s. Control experiments (OCP data) were not significantly different than the original feed samples, indicating that adsorption was minimal. In general, results show the accumulation of shorter chain PFAS (e.g., PFBS, PFHpA, PFHxS), presumably from the oxidation of longer chain PFAS (e.g., PFNA, PFOS). At the highest cell potentials tested (e.g., 8.1 and 10.5 V) total PFAS removal was ~50% (**Figure E3**). The lack of total removal of PFAS was attributed to the presence of background organic compounds (chemical oxidant demand (COD) = 43.3 mg/L) and low solution conductivity (**Table E1**). The background organic compounds can compete with PFAS for reactive sites on the REM, and the low conductivity caused a significant potential drop in solution and therefore reduced the reactive thickness of the REM.

Table E1. General Water Quality Analyses for Groundwater Samples.

	GW1	GW2
Constituent	**mg/L**	**mg/L**
F^-	1.06	15.7
Cl^-	51.5	27.1
NO_3^-	8.18	175
SO_4^{2-}	10.8	< 0.1
HPO_4^{2-}	7.78	< 0.1
HCO_3^-	228	87.7
Na^+	72.6	25.3
K^+	13.7	30.1
Ca^{2+}	25.7	34.5
Mg^{2+}	21.4	8.75
pH	6.8	6.5
Conductivity (µS/cm)	788	337
COD (mg/L)	43.3	4.35
Alkalinity (mg/L $CaCO_3$)	373	144

The GW2 sample was obtained from Willow Grove Naval Base in collaboration with Jason Speicher. The general water quality parameters are shown in **Table 1** and PFAS concentrations are shown in **Figure E4a** (Feed/OCP data). Control experiments (OCP data) were not significantly different than the original feed samples, indicating that adsorption was minimal. Operation of the REM in single-pass mode with a low flux (J = 60 LMH) resulted in approximately 55% total PFAS

removal (**Figure E3a**). Once again, longer chain PFAS were oxidized to shorter chain PFAS, and the background COD and low conductivity inhibited complete oxidation. In order to increase the oxidation rate, the operational mode of the REM was switched to recycle mode. In this mode of operation, the solution was continuously recycled through the REM until the target removal was achieved. A flux (J = 720 LMH) was chosen that corresponded to the maximum rate observed for PFOA/PFOS oxidation experiments (see **Figure E2b**). Individual final PFAS concentrations were < 61 ng/L and total PFAS concentrations were 274 ng L^{-1} (**Figure E4b**). The percent removals for individual and total PFAS are shown in **Figure E5** and indicate that total PFAS destruction was > 99%. These results indicate that a recycle mode operation with high flux is needed to improve mass transfer and increase contact time with the REM, which resulted in effective oxidation of PFAS in the groundwater solution. ***These experiments achieved both Milestones 2 and 3, as stated above.***

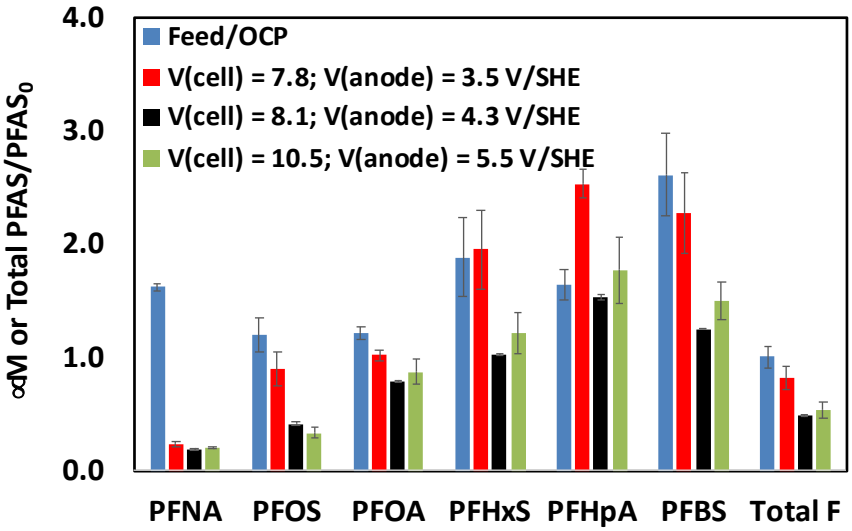

Figure E3. PFAS and Total F Removal in GW1 Sample as a Function of Cell Potential.

J = 60 LMH

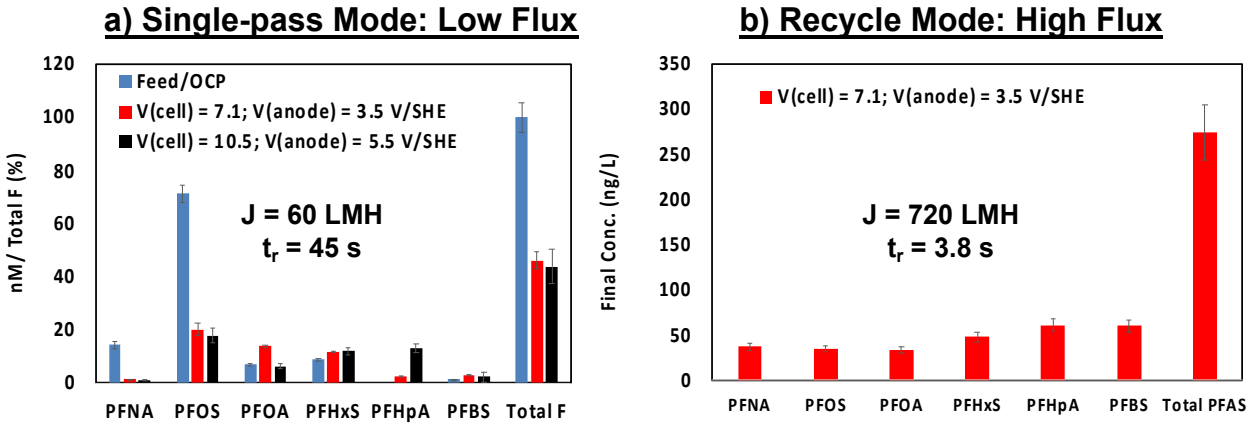

Figure E4. Comparison of Electrochemical Oxidation of PFAS in GW2 in Single-Pass Versus Recycle Modes.

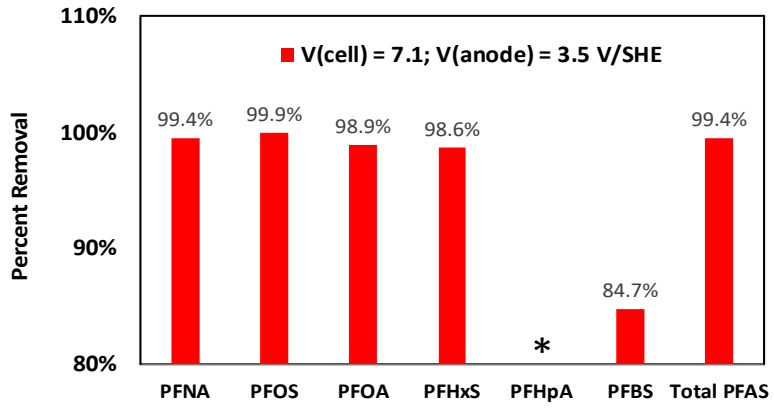

Figure E5. Percent Removal of PFAS Compounds in GW2.

**PFHpA was not detected in the feed solution, but was produced during treatment to a final concentration of 60 ng/L.*

4.4 ENERGY REQUIREMENTS

Work in this section focused on addressing **Milestone 4: Determination of the energy costs for achieving the 70 ng L^{-1} treatment goal in PFAS-contaminated groundwater with a target energy usage of < 2.0 kWh m^{-3} (per log removal) of water treated.**

A key issue associated with destructive PFAS remediation technologies is the operational cost. While a complete analysis of operating costs for PFAS remediation technologies could not be found in the existing literature, the project team has recently summarized the energy consumption per log-removal for various novel technologies for PFOA/PFOS degradation (Le et al. 2019), which is also summarized in **Appendix A**. Remediation technologies that were reviewed include sonolysis (Vecitis et al. 2008; Cheng et al. 2010; Schroder and Meesters 2005; Lin at al. 2016), microwave-hydrothermal (Lee et al. 2009), photolysis (Hori et al. 2004; Chen et al. 2007; Lyu et al. 2015), photocatalysis (Li et al. 2012a; Li et al. 2012b; Huang et al. 2016), and electrochemical oxidation (Niu et al. 2012; Ochiai et al. 2011; Le et al. 2019; Schaefer et al. 2017; Schaefer et al. 2015; Zhou et al. 2017; Xu et al. 2017; Lin et al. 2012; Zhuo et al. 2011; Yang et al. 2015; Zhao et al. 2013; Lin et al. 2018). Direct electrochemical oxidation of PFAS is by far the most energy efficient destructive method reported to date (5 – 132 kWh m^{-3}) (Le et al. 2019; Schaefer et al. 2017; Lin et al. 2018; Niu et al. 2016). Porous Magnéli phase Ti_4O_7 ceramic anodes have shown the lowest energy consumption of 5 kWh/m^3 for PFOA and between 6.7 to 32 kWh/m^3 for PFOS (Le et al. 2019; Lin et al. 2018), further demonstrating the promise of this technology. In this study, the electrode energy requirements for the Ti_4O_7 REM anode to remove 10 µM initial concentrations of PFOA and PFOS to below the detection limits (86 ng L^{-1} for PFOA and 35 ng L^{-1} for PFOS) were 5.1 ± 0.1 and 6.7 ± 0.2 kWh m^{-3}, respectively. Additionally, it was found that the groundwater samples required 13-24 kWh m^{-3} to treat GW1 and 11-15 kWh m^{-3} to treat GW2 in single-pass mode. The energy usage decreased to 2.9 kWh m^{-3} to treat GW2 in recycle mode, which was able to decrease individual PFAS to < 61 ng/L. Although the lowest energy consumption observed during this project (i.e., 2.9 kWh m^{-3}) was 45% higher than the 2.0 kWh m^{-3} goal, this energy consumption value is the lowest reported in the literature and shows the extreme promise of the REM technology.

Further optimization of reactor design and operation will undoubtedly lower the energy consumption of the REM.

5.0 RESEARCH AND BENEFITS

The high rate constants reported above are the highest reported for electrochemical oxidation of PFAS, and the low energy consumptions are much more favorable then other destructive treatment technologies (i.e, ultrasonication, photocatalysis, vacuum UV photolysis, microwave-hydrothermal decomposition), demonstrating the promise of the REM technology for PFAS treatment. In order to determine the full feasibility of this technology, further research and development is needed, which includes 1) reactor scale-up/optimization; 2) impact of co-contaminants; 3) longevity studies; and 4) life cycle and cost assessments. Completion of this follow-on research is needed before the REM technology can be confidently deployed to remediation sites.

6.0 LITERATURE CITED

Association of State Drinking Water Administrators (ASDWA), Per- and Polyfluoroalkyl Substances (PFAS). https://www.asdwa.org/pfas/ (accessed 6 July 2020).

Carter, K.E. and Farrell, J. (2010). Removal of Perfluorooctane and Perfluorobutane Sulfonate from Water via Carbon Adsorption and Ion Exchange. *Separation Science and Technology,* 45(6), 762-767.

Chen, J., Zhang, P.Y. and Liu, J. (2007). Photodegradation of perfluorooctanoic acid by 185 nm vacuum ultraviolet light. *Journal of Environmental Sciences*, 19(4), 387-390.

Chen, M.-J., Lo, S.-L., C.-H., Lee, Y.-C., Kuo, J. and Wu, C.-H. (2016). Decomposition of Perfluorooctanoic Acid by Ultraviolet Light Irradiation with Pb-Modified Titanium Dioxide. *J. Hazard. Mater.,* 303, 111-118.

Cheng, J., Vecitis, C.D., Park, H., Mader, B.T., Hoffmann, M.R. (2010). Sonochemical Degradation of Perfluorooctane Sulfonate (PFOS) and Perfluorooctanoate (PFOA) in Groundwater: Kinetic Effects of Matrix Inorganics. *Environmental Science & Technology*, 44(1), 445-450.

EPA (2016). Drinking Water Health Advisory for Perfluorooctanoic Acid (PFOA). EPA 822-R-16-005. Washington, D,C. Retrieved October 2018 from https://www.epa.gov/sites/production/files/2016-05/documents/pfoa_health_advisory_final_508.pdf.

Eschauzier, C., Beerendonk, E., Scholte-Veenendaal, P. and De Voogt, P. (2012). Impact of Treatment Processes on the Removal of Perfluoroalkyl Acids from the Drinking Water Production Chain. *Environmental Science & Technology*, 46(3), 1708-1715.

Hori, H., Hayakawa, E., Einaga, H., Kutsuna, S., Koike, K., Ibusuki, T., Kiatagawa, H. and Arakawa, R. (2004). Decomposition of environmentally persistent perfluorooctanoic acid in

water by photochemical approaches. *Environmental Science & Technology*, 38(22), 6118-6124.

Huang, J.Y., Wang, X., Pan, Z.Q., Li, X.K., Ling, Y. and Li, L.S. (2016). Efficient degradation of perfluorooctanoic acid (PFOA) by photocatalytic ozonation. *Chemical Engineering Journal*, 296, 329-334.

Jin, L. and Zhang, P. (2015). Photochemical Decomposition of Perfluorooctane Sulfonate (PFOS) in an Anoxic Alkaline Solution by 185 nm Vacuum Ultraviolet. *Chem. Eng. J.*, 280, 241-247.

Le, T.X.H., Haflich, H., Shah, A.D. and Chaplin, B.P. (2019). Energy-Efficient Electrochemical Oxidation of Perfluoroalkyl Substances using a Ti_4O_7 Reactive Electrochemical Membrane Anode. *Environ. Sci. Technol. Lett.*, 6(8), 504-510.

Lee, Y.C., Lo, S.L., Chiueh, P.T. and Chang, D.G. (2009). Efficient decomposition of perfluorocarboxylic acids in aqueous solution using microwave-induced persulfate. *Water Research*, 43(11), 2811-2816.

Li, X.Y., Zhang, P.Y., Jin, L., Shao, T., Li, Z.M. and Cao, J.J. (2012a). Efficient Photocatalytic Decomposition of Perfluorooctanoic Acid by Indium Oxide and Its Mechanism. *Environmental Science & Technology*, 46(10), 5528-5534.

Li, Z.M., Zhang, P.Y., Shao, T. and Li, X.Y. (2012b). In_2O_3 nanoporous nanosphere: A highly efficient photocatalyst for decomposition of perfluorooctanoic acid. *Applied Catalysis B-Environmental*, 125, 350-357.

Lin, H., Niu, J., Ding, S. and Zhang, L. (2012). Electrochemical degradation of perfluorooctanoic acid (PFOA) by Ti/SnO_2-Sb, Ti/SnO_2-Sb/PbO_2 and Ti/SnO_2-Sb/MnO_2 anodes. *Water Research*, 46(7), 2281-2289.

Lin, H., Niu, J., Liang, S., Wang, C., Wang, Y., Jin, F., Luo, Q. and Huang, Q. (2018). Development of Macroporous Magnéli Phase Ti_4O_7 Ceramic Materials: As an Efficient Anode for Mineralization of Poly- and Perfluoroalkyl Substances. *Chem. Eng. J.*, 354, 1058-1067.

Lin, J.C., Hu, C.Y. and Lo, S.L. (2016). Effect of surfactants on the degradation of perfluorooctanoic acid (PFOA) by ultrasonic (US) treatment. *Ultrasonics Sonochemistry,* 28, 130-135.

Lyu, X.J., Li, W.W., Lam, P.K.S. and Yu, H.Q. (2015). Boiling significantly promotes photodegradation of perfluorooctane sulfonate. *Chemosphere*, 138, 324-327.

Niu, J., Li, Y., Shang, E., Xu, Z. and Liu, J. (2016). Electrochemical oxidation of perfluorinated compounds in water. *Chemosphere*, 146, 526-38.

Niu, J., Lin, H., Gong, C. and Sun, X. (2013). Theoretical and Experimental Insights into the Electrochemical Mineralization Mechanism of Perfluorooctanoic Acid. *Environ. Sci.Technol.*, 47(24), 14341-14349.

Niu, J., Lin, H., Xu, J., Wu, H. and Li, Y. (2012). Electrochemical Mineralization of Perfluorocarboxylic Acids (PFCAs) by Ce-Doped Modified Porous Nanocrystalline PbO_2 Film Electrode. *Environmental Science & Technology,* 46(18), 10191-10198.

Ochiai, T., Iizuka, Y., Nakata, K., Murakami, T., Tryk, D.A., Fujishima, A., Koide, Y. and Morito, Y. (2011). Efficient electrochemical decomposition of perfluorocarboxylic acids by the use of a boron-doped diamond electrode. *Diamond and Related Materials*, 20(2), 64-67.

Pramanik, B.K., Pramanik, S.K. and Suja, F. (2015). A comparative study of coagulation, granular- and powdered-activated carbon for the removal of perfluorooctane sulfonate and perfluorooctanoate in drinking water treatment. *Environmental Technology*, 36(20), 2610-2617.

Schaefer, C.E., Andaya, C., Burant, A., Condee, C.W., Urtiaga, A., Strathmann, T.J. and Higgins, C.P. (2017). Electrochemical treatment of perfluorooctanoic acid and perfluorooctane sulfonate: Insights into mechanisms and application to groundwater treatment. *Chemical Engineering Journal*, 317, 424-432.

Schaefer, C.E., Andaya, C., Urtiaga, A., McKenzie, E.R. and Higgins, C.P. (2015). Electrochemical treatment of perfluorooctanoic acid (PFOA) and perfluorooctane sulfonic acid (PFOS) in groundwater impacted by aqueous film forming foams (AFFFs). *Journal of Hazardous Materials*, 295, 170-175.

Schroder, F. and Meesters, R. (2005) Stability of fluorinated surfactants in advanced oxidation processes: A follow up of degradation products using flow injection-mass spectrometry, liquid chromatography-mass spectrometry and liquid chromatography-multiple stage mass spectrometry. *J. Chromatogr. A.*, 1082, 110-119.

Schroder, H.F. and Meesters, R.J.W. (2005). Stability of fluorinated surfactants in advanced oxidation processes - A follow up of degradation products using flow injection-mass spectrometry, liquid chromatography-mass spectrometry and liquid chromatography-multiple stage mass spectrometry. *Journal of Chromatography A*, 1082(1), 110-119.

Vecitis, C.D., Park, H., Cheng, J., Mader, B.T. and Hoffmann, M.R. (2008). Enhancement of Perfluorooctanoate and Perfluorooctanesulfonate Activity at Acoustic Cavitation Bubble Interfaces. *Journal of Physical Chemistry C*, 112(43), 16850-16857.

Xu, Z., Yu, Y., Liu, H. and Niu, J. (2017). Highly Efficient and Stable Zr-Doped Nanocrystalline PbO2 Electrode for Mineralization of Perfluorooctanoic Acid in a Sequential Treatment System. *Sci. Total Environ.*, 579, 1600-1607.

Yang, B., Jiang, C.J., Yu, G., Zhuo, Q.F., Deng, S.B., Wu, J.H. and Zhang, H. (2015). Highly efficient electrochemical degradation of perfluorooctanoic acid (PFOA) by F-doped Ti/SnO_2 electrode. *Journal of Hazardous Materials*, 299, 417-424.

Yao, Y., Volchek, K., Brown, C.E., Robinson, A. and Obal, T. (2014). Comparative study on adsorption of perfluorooctane sulfonate (PFOS) and perfluorooctanoate (PFOA) by different adsorbents in water. *Water Science and Technology*, 70(12), 1983-1991.

Yu, Q., Zhang, R.Q., Deng, S.B., Huang, J. and Yu, G. (2009). Sorption of perfluorooctane sulfonate and perfluorooctanoate on activated carbons and resin: Kinetic and isotherm study. *Water Research*, 43(4), 1150-1158.

Zhang, D., Luo, Q., Gao, B., Chiang, S.-Y.D., Woodward, D. and Huang, Q. (2016). Sorption of perfluorooctanoic acid, perfluorooctane sulfonate and perfluoroheptanoic acid on granular activated carbon. *Chemosphere*, 144, 2336-2342.

Zhao, D., Cheng, J., Vecitis, C.D. and Hoffmann, M.R. (2011). Sorption of Perfluorochemicals to Granular Activated Carbon in the Presence of Ultrasound. *J. Phys. Chem. A*, 115(11), 2250-2257.

Zhao, H., Gao, J., Zhao, G., Fan, J., Wang, Y. and Wang, Y. (2013). Fabrication of Novel SnO_2-Sb/carbon Aerogel Electrode for Ultrasonic Electrochemical Oxidation of Perfluorooctanoate with High Catalytic Efficiency. *Appl. Catal. B Environ.*, 136–137, 278–286.

Zhuo, Q. F., Xiang, Q., Yi, H., Zhang, Z.K., Yang, B., Cui, K., Bing, X.Y., Xu, Z.C., Liang, X.L., Guo, Q.W. and Yang, R. (2017). Electrochemical oxidation of PFOA in aqueous solution using highly hydrophobic modified PbO2 electrodes. *Journal of Electroanalytical Chemistry*, 801, 235-243.

Zhuo, Q., Deng, S., Yang, B., Huang, J. and Yu, G. (2011). Efficient Electrochemical Oxidation of Perfluorooctanoate Using a Ti/SnO_2-Sb-Bi Anode. *Environmental Science & Technology*, 45(7), 2973-2979.

APPENDIX A COMPARISON OF ENERGY CONSUMPTION OF REPORTED TECHNOLOGIES FOR PFOA/PFOS DEGRADATION

Energy usage calculated per log removal.

Technique	Conc. (mg L^{-1})	Experimental Conditions	Removal efficiency of PFAS	*Energy usage (kWh m^{-3})*	Ref.
		PFOA			
Sonolysis	0.01	358 kHz, power density of 250 W L^{-1}, 10 ^{0}C,	100 % in 150 min	***208***	1
Sonolysis	10	200W, 20 ^{0}C, argon atmosphere	85 % in 60 min	***4045***	2
Sonolysis	0.1	354 kHz, power density of 250 W L^{-1}, 10 ^{0}C, argon atmosphere	95 % in 140 min	***448***	3
Microwave / $S_2O_8^{2-}$	105	70 W, 90 ^{0}C, 50 mM $S_2O_8^{2-}$	99.3 % in 4 h	***2599***	4
Ultrasonication/ CTAB	50	150 W, 40 kHz, 25 ^{0}C, 0.12 mM CTAB	79 % in 2 h	***1475***	5
Photolysis	559	pH = 3.7, N_2 atm., λ = 254 nm, 200 W	89.5 % in 72 h	***6687243***	6
Photolysis	41	pH = 3.7, 40 ^{0}C, N_2 atm., λ = 185 nm, 15 W	61.7 % in 2 h	***90***	7
Photocatalysis/In_2O_3	41	pH = 4, 0.5 g L^{-1} In_2O_3, 25 ^{0}C, λ = 254 nm, 23 W	82 % in 4 h	***309***	8
Photocatalysis/In_2O_3	30	pH = 3.9, 0.5 g L^{-1} In_2O_3, 25 ^{0}C, λ = 254 nm, 23 W	100 % in 3 h	***230***	9
Photocatalysis/sulfite	8.3	pH = 10.3, 25 ^{0}C, N_2 atm., λ = 254 nm, $[SO_3^{2-}]_0$ = 10 mM, 10 W	100 % in 24 h	***400***	10
Photocatalysis/sulfite	16	pH = 9.2, $[SO_3^{2-}]_0$ = 10 mM, $[DO]_0$ = ~5 mg L^{-1}, 250W	100 % in 10 min	***556***	11
Photocatalysis/sulfite	8.3	pH = 10.3, 25 ^{0}C, N_2 atm., λ = 254 nm, $[SO_3^{2-}]_0$ = 10 mM, 10 W	100 % in 24 h	***400***	10
Photocatalysis/sulfite	16	pH = 9.2, $[SO_3^{2-}]_0$ = 10 mM, $[DO]_0$ = ~5 mg L^{-1}, 250W	100 % in 10 min	***556***	10
Photocatalysis/Carbonate	50	pH = 8.96–8.3, 40 mM HCO_3-, 0.075% H_2O_2, λ = 254 nm, 400 W	100 % in 12 h	***800***	12
Photocatalysis/$S_2O_8^{2-}$	559	pH = 2–3, 50 mM $S_2O_8^{2-}$, λ = 254 nm, 200 W	100 % in 4 h	***12121***	13
Photocatalysis/Cu–TiO_2	50	pH = 5, 0.5 g L^{-1}, Cu–TiO_2, λ = 254 nm, 400 W	91% in 12 h	***4173***	14
Photocatalysis/Pb–TiO_2	50	pH = 5, 0.5 g L^{-1}, Pb–TiO_2, λ = 254 nm, 400 W	99.9 % in 12 h	***1455***	15
Photocatalysis/Pt–TiO_2	60	pH = 3, 0.5 g L^{-1}, Pt–TiO_2, λ = 365 nm, 125 W	100 % in 7 h	***1458***	16
Photocatalysis/TiO_2-MWCNT	30	pH = 5, 1.6 g L^{-1}, TiO_2-MWCNT, λ = 365 nm, 300 W	94 % in 8 h	***7857***	17
Photocatalysis/TiO_2-O_3	10	0.2 g TiO_2, 25 mg h^{-1} O_3, λ = 254 nm, 28 W	100 % in 4 h	***37***	18
Photocatalysis/TiO_2-rGO	100	pH = 3.8, 0.1 g L^{-1} TiO_2-rGO, 150 W	93 % in 12 h	***1559***	19

Technique	Conc. (mg L^{-1})	Experimental Conditions	Removal efficiency of PFAS	*Energy usage (kWh m^{-3})*	Ref.
Photocatalysis/TiO_2-Oxalic acid	10	0.5 g L^{-1} TiO_2, 3 mM $H_2C_2O_4$, N_2 atm., λ = 254 nm, 23 W	86.7 % in 3 h	***158***	20
Photocatalysis/Fenton	8.3	pH = 3, 32 mM H_2O_2, 2 mM Fe^{2+}, λ = 254 nm, 9 W	95.2 % in 5 h	***171***	21
Photocatalysis/SiC/Graphene	50	pH = 7.0, 0.5 g L^{-1}, λ = 254 nm, 5 W	58.5 % in 8 h	***1309***	22
Photocatalysis/KI	10	0.3 mM KI, N_2 atm., pH = 9.0, λ = 254 nm, 15 W	100 % in 14 h	***95***	23
Photocatalysis/β-Ga_2O_3	31	pH = 4.8, 0.5 g L^{-1} β-Ga_2O_3, 2 mM Fe^{2+}, λ = 254 nm, 15 W	98.8 % in 3 h	***234***	24
Echem. Oxid.	100	Zr-PbO_2 anode, current density = 10 mA cm^{-2}	97 % in 90 min	***44***	25
Echem. Oxid.	100	Ti/SnO_2–Sb/PbO_2 anode, current density = 10 mA cm^{-2}	91.1 % in 90 min	***96***	26
Echem. Oxid.	100	pH = 3, Ti/SnO_2-Sb_2O_5/PbO_2-PVDF (1.0 wt%) anode, current density = 40 mA cm^{-2}	92.1 % in 180 min	***144***	27
Echem. Oxid.	50	Ti/SnO_2-Sb-Bi anode, current density, power density of 13.04 W L^{-1}	99 % in 2 h	***13***	28
Echem. Oxid.	100	Ce-PbO_2 anode, current density = 20 mA cm^{-2}	96.7 % in 90 min	***30***	29
Echem. Oxid.	100	Ti/SnO_2-F anode, current density = 20 mA cm^{-2}	99 % in 30 min	***45***	30
Ultrasonic Echem. Oxid.	100	SnO_2-Sb/Carbon anode, current density = 20 mA cm^{-2}, 33 kHz, 50W	91 % in 5 h	***3985***	31
Echem. Oxid.	207	Ti_4O_7 anode, current density = 5 mA cm^{-2}	> 99.9 % in 2 h	***5***	32
Echem. Oxid.	15	BDD anode, current density = 15 mA cm^{-2}	> 90 % in 8 h	***113***	33
Echem. Oxid.	0.013	Ti/RuO_2 anode, current density = 10 mA cm^{-2}	~ 95 % in 8 h	***76***	34
Echem. Oxid.	4.14	Ti_4O_7 REM anode, V anode = 3.3 V/SHE	> 99.9 % at *J* = 240 LMH	***5.1***	***Present study***
PFOS					
Sonolysis	0.01	358 kHz, power density of 250 W L^{-1}, 10 ^{0}C,	98 % in 180 min	***441***	1
Sonolysis	10	200W, 20 ^{0}C, argon atmosphere	48 % in 58 min	***11345***	2
Sonolysis	0.1	354 kHz, power density of 250 W L^{-1}, 10 ^{0}C, argon atmosphere	72 % in 140 min	***1055***	3
Boiling	18.6	pH = 7, 102 ^{0}C, 6 mM PBS, 25 mL min^{-1} O_2/N_2, λ = 254 nm, 500 W	98 % in 4 h	***1177***	35
Photolysis	20	38-50 ^{0}C, N_2 atm., λ = 254 nm, 32 W	68 % in 10 days	***20693***	36
Photocatalysis/Alkaline 2-propanol	20	38-50 ^{0}C, 90 μM NaOH, N_2 atm., λ = 254 nm, 32 W	92 % in 10 days	***9335***	36
Photolysis	18.6	100 ^{0}C, pH = 11.8, λ = 254 nm, 500 W	99.8 % in 4 h	***3705***	37

Technique	Conc. (mg L^{-1})	Experimental Conditions	Removal efficiency of PFAS	*Energy usage (kWh m^{-3})*	Ref.
Photolysis	10	25 ^{0}C, pH = 12.8, λ = 185 nm, 23 W	95.3 % in 72 h	***3118***	38
Echem. Oxid.	50	Ti_4O_7 anode, current density = 5 mA cm^{-2}	93.1 % in 3 h	***32***	32
Echem. Oxid.	46.45	Ti/TiO_2-NTs/Ag_2O/PbO_2 anode, current density = 30 mA cm^{-2}	74.87 % in 3h	***65***	39
Echem. Oxid.	0.018	Ti/RuO_2 anode, current density = 10 mA cm^{-2}	~ 95 % in 8 h	***76***	34
Echem. Oxid.	5	Ti_4O_7 REM anode, V anode = 3.6 V/SHE	> 99.9 % at *J* = 240 LMH	***6.7***	***Present study***

atm. = atmosphere
CTAB = Hexadecyl trimethyl ammonium bromide
DO = Dissolved Oxygen
Echem. Oxid. = Electrochemical Oxidation
PVDF = Polyvinylidene Fluoride
PBS = Phosphate Buffer Solution